第32卷第6期
2013年12月

红外与毫米波学报
J. Infrared Millim. Waves

Vol. 32, No. 6
December, 2013

文章编号:1001-9014(2013)06-0481-06

DOI:10.3724/SP.J.1010.2013.00481

Effects of compositional overshoot on InP-based InAlAs metamorphic graded buffer

FANG Xiang[1,3], GU YI[1,2], ZHANG Yong-Gang[1,2*], ZHOU Li[1,3], WANG Kai[1], LI Hao-Si-Bai-Yin[1], LIU Ke-Hui[1,3], CAO Yuan-Ying[1,3]

(1. State Key Laboratory of Functional Materials for Informatics, Shanghai Institute of Microsystem and Information Technology, Chinese Academy of Sciences, Shanghai 200050, China
2. Key Laboratory of Infrared Imaging Materials and Detectors, Chinese Academy of Sciences, Shanghai 200083, China
3. Graduate School of Chinese Academy of Sciences, Beijing 100049, China)

Abstract: $In_{0.78}Ga_{0.22}As/In_{0.78}Al_{0.22}As$ quantum wells and $In_{0.84}Ga_{0.16}As$ photodetctor samples have been grown on InP-based $In_xAl_{1-x}As$ metamorphic graded buffers to investigate the effects of compositional overshoot on the material characteristics. Atomic force microscopy results show that the surface roughness is reduced by the compositional overshoot in the InAlAs buffer layers for both the quantum well and photodetector samples. In the case of thin quantum wells, X-ray diffraction reciprocal space mapping and photoluminescence measurements show that the use of compositional overshoot can increase the relaxation degree, reduce the residual strain and improve the optical quality. While in the case of thicker photodetectors, no obvious improvement is observed after using compositional overshoot. The different behaviours of the metamorphic quantum wells and photodetectors should be considered in the device applications.

Key words: InAlAs, buffer, X-ray diffraction, photoluminescence

PACS: 81.15.Hi, 81.05.Ea, 61.05.cp

组分过冲对 InP 基 InAlAs 递变缓冲层的影响

方 祥[1,3], 顾 溢[1,2], 张永刚[1,2*], 周 立[1,3],
王 凯[1], 李好斯白音[1], 刘克辉[1,3], 曹远迎[1,3]

(1. 中国科学院上海微系统与信息技术研究所 信息功能材料国家重点实验室,上海 200050;
2. 中国科学院红外成像材料与器件重点实验室,上海 200083;
3. 中国科学院研究生院,北京 100049)

摘要:通过在 InP 基 $In_xAl_{1-x}As$ 递变缓冲层上生长 $In_{0.78}Ga_{0.22}As/In_{0.78}Al_{0.22}As$ 量子阱和 $In_{0.84}Ga_{0.16}As$ 探测器结构,研究了缓冲层中组分过冲对材料特性的影响.原子力显微镜结果表明,在 InAlAs 缓冲层中采用组分过冲可以使量子阱及探测器样品表面粗糙度都得到降低.对于相对较薄的量子阱结构,X 射线衍射倒易空间扫描图和光致发光谱的测量表明,使用组分过冲可以增加弛豫度、减小剩余应力并改善光学性质.而对于较厚的探测器结构,X 射线衍射和光致发光谱测试发现使用组分过冲后的材料性质没有明显的变化.量子阱和探测器结构的这些不同特性需要在器件设计应用中加以考虑.

关 键 词:InAlAs;缓冲层;X 射线衍射;光致发光

中图分类号:TN2 **文献标识码**:A

Received date: 2012-08-04, **revised date**: 2013-04-01 **收稿日期**:2012-08-04, **修回日期**:2013-04-01

Foundation items: National Basic Research Program of China (2012CB619202), the Founding of CAS Key Laboratory of Infrared Imaging Materials and Detectors, and Innovative Founding of Shanghai Institute of Microsystem and Information Technology, CAS.

Biography: FANG Xiang, (1986-), male, Hubei Huanggang, Ph. D. candidate, research area is optoelectronic materials and devices. E-mail: xfang@mail.sim.ac.cn

* **Corresponding author**: E-mail: ygzhang@mail.sim.ac.cn

Introduction

Metamorphic growth has shown great potential in fabricating high performance specific devices on conventional substrates. By using the metamorphic growth, the lack of large and high-quality commercial substrates with desired lattice constants can be partly overcome, which significantly favors the designs of device structures. However, the generation of dislocations and the degradation of crystalline are always accompanied with the metamorphic growth. Accordingly, a suitable buffer layer between the substrate and the active layers is required. An appropriate buffer layer should relax the strain sufficiently, prevent the propagation of threading dislocations (TDs) formed during the relaxation process into the active layers, and form a moderate smooth surface morphology suitable for further device processing. Various techniques have been implemented in the metamorphic growth, such as the use of a thick uniform buffer[1], continuously graded[2-3] or step graded buffer[4-5]. In addition, Be-doped buffer[6], dilute nitride buffer[7] and the insertion of a built-in strain field[8] or digital alloy[9] have also been adopted to decrease the TD density. Considering the convenience of practical operation during the growth, reliability and reproducibility of the devices, the compositionally graded buffer is an easy and effective approach for metamorphic growth.

It was proposed that a dislocation-free portion will be formed when the thickness of the buffer is excess of a value of Z_c in the linearly graded buffer. The value of Z_c can be expressed as [10]

$$Z_c = W - (2\lambda/bc\varepsilon')^{1/2} \quad , \quad (1)$$

where W is the total thickness of the buffer, λ is the energy per unit length of the dislocation, c is the appropriate elastic constant for biaxial strain, b is the misfit component of the Burgers vector of dislocation, and ε' is the grading rate of mismatch. The residual strain in this dislocation-free portion is

$$\bar{\varepsilon} = W\varepsilon' - Z_c\varepsilon' = (2\lambda\varepsilon'/bc)^{1/2} \quad . \quad (2)$$

In the linearly graded buffer, an "overshoot" of the mismatch by an amount $\bar{\varepsilon}$ is needed to make the graded buffer lattice matched with the following layers.

InAlAs metamorphic buffers are very suitable for the growth of high indium composition metamorphic optoelectronic structures on GaAs and InP substrates, including both laser diodes and photodetectors (PDs)[11]. Many investigations on InAlAs buffers were performed on the samples grown on GaAs substrate [12-13], whereas there are few studies of the InAlAs metamorphic buffers on InP substrate [9,11]. In this letter, InGaAs/InAlAs quantum wells (QWs) and InGaAs PD structures with high indium composition are grown on InP-based $In_xAl_{1-x}As$ metamorphic graded buffers. The effects of the compositional overshoot in the $In_xAl_{1-x}As$ linearly graded buffers on the material properties have been investigated in detail.

1 Experiments

The samples grown in this work were performed on the (001)-oriented InP epi-ready substrates by a VG Semicon V80H gas source molecular beam epitaxy (GSMBE) system. The elemental indium, gallium and aluminum sources were used as group III sources, and their fluxes were controlled by changing the temperatures of cells. Arsine and phosphine cracking cells were used as group V sources, and the fluxes were controlled by adjusting the pressure. The cracking temperature was about 1000℃ measured by thermocouple. Standard beryllium and silicon effusion cells were used as p- and n-type doping sources, and the doping levels were also controlled by changing the temperatures of sources. The surface oxide desorption of the substrate was carried out under P_2 flux, including a slow ramp-up of the substrate temperature until the reflection high energy electron diffraction (RHEED) pattern showed an abrupt transformation to 2×4 surface reconstruction.

To investigate the effects of compositional overshoot in $In_xAl_{1-x}As$ graded buffers, two $In_{0.78}Ga_{0.22}As/In_{0.78}Al_{0.22}As$ QW samples (samples 1 and 2) and two $In_{0.84}Ga_{0.16}As$ PD samples (samples 3 and 4) were grown. As shown in Fig. 1, the growth of the QW samples started with a 100 nm InP buffer, followed by a 1.7 μm $In_xAl_{1-x}As$ graded metamorphic buffer through the simultaneous increase of indium source temperature and decrease of aluminum source temperature. In the $In_xAl_{1-x}As$ buffer, the indium composition

x was designed grading from 0.52 to 0.78 for sample 1, and from 0.52 to 0.82 for sample 2 as shown in Figs. 1(a) and 1(b), respectively. At last, three 10 nm $In_{0.78}Ga_{0.22}As$ QWs sandwiched by $In_{0.78}Al_{0.22}As$ barriers were grown. The thicknesses of $In_{0.78}Al_{0.22}As$ barriers between the well layers were 12 nm, while the thicknesses of the first and last barriers were 100 nm. The $In_{0.84}Ga_{0.16}As$ PD structures contain a 200 nm highly Be-doped p^+ InP buffer, a 100 nm highly Be-doped p^+ $In_{0.52}Al_{0.48}As$ buffer, a 1.76 μm highly Be-doped p^+ $In_xAl_{1-x}As$ graded buffer, a 72 nm $In_{0.84}Ga_{0.16}As/In_{0.84}A_{10.16}As$ digital graded superlattice (DGSL)[14], a 2.0 μm slightly Si-doped $In_{0.84}Ga_{0.16}As$ absorption layer, and at last a 0.25 μm highly Si-doped $In_{0.84}Ga_{0.16}As$ contact layer. In the $In_xAl_{1-x}As$ buffer, the indium composition x was designed grading from 0.52 to 0.84 for sample 3, and from 0.52 to 0.88 for sample 4 as shown in Figs. 1(c) and 1(d), respectively. Therefore, for sample 2 and 4, there is an indium compositional overshoot of 0.04 in the end of $In_xAl_{1-x}As$ buffer layers with respect to the following epilayers on the buffers.

After the growth, the surface of the samples were observed by an atomic force microscopy (AFM). In order to characterize the structural properties of all the samples, X-ray diffraction reciprocal space mapping (RSM) measurement was performed for the symmetric (004) and asymmetric (224) reflections by a Philips X' pert MRD high resolution X-ray diffractometer (HRXRD) equipped with a four-crystal Ge (220) monochrometer. The optical properties of the samples were investigated by the measurements of the room temperature (RT) photoluminescence (PL) spectra. The measurements were performed by a Nicolet Megna 860 Fourier transform infrared (FTIR) spectrometer, in which a liquid-nitrogen cooled InSb detector and a CaF2 beam splitter were applied. A diode-pumped solid-state (DPSS) laser with the wavelength of 1064 nm was used as the exciting source. The optical paths and other measurement conditions are kept unchanged during the measurement; therefore, the PL intensities of various samples can be compared.

2　Results and discussion

The surface images observed by AFM in the tapping mode are shown in Fig. 2. The scan area for each sample is 40 μm × 40 μm. All the samples show ob-

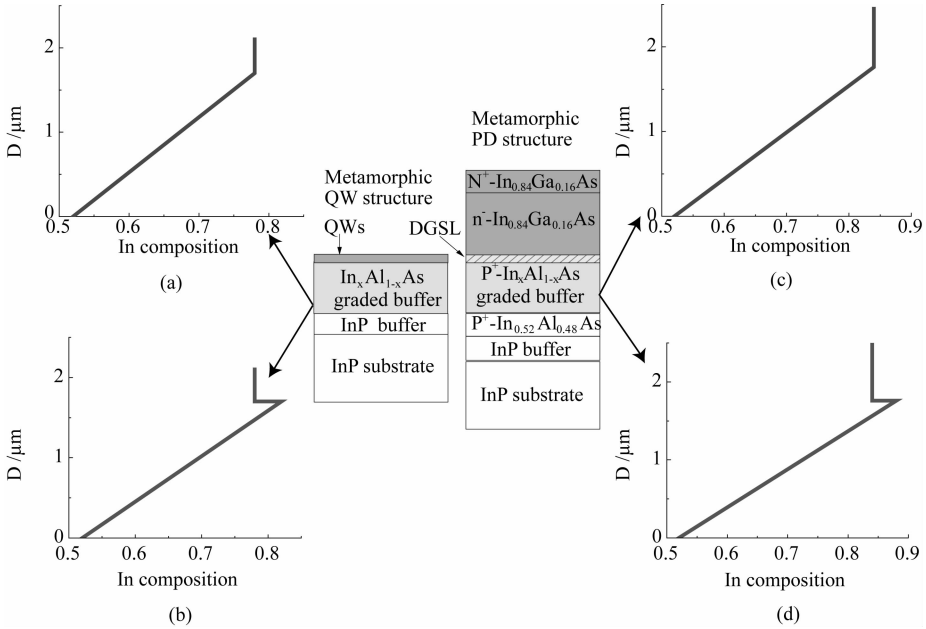

Fig. 1　The schematic structures of $In_{0.78}Ga_{0.22}As/In_{0.78}Al_{0.22}As$ QW samples and $In_{0.84}GA_{0.16}As$ PD samples grown on InP-based $In_xAl_{1-x}As$ metamorphic graded buffers. (a), (b), (c) and (d) refer to the indium composition profile versus the thickness of InAlAs buffer layer in samples 1, 2, 3 and 4 respectively

图 1　InP 基 $In_xAl_{1-x}As$ 递变递变缓冲层上的 $In_{0.78}Ga_{0.22}As/In_{0.78}Al_{0.22}As$ 量子阱和 $In_{0.84}GA_{0.16}As$ 探测器的结构示意图. 图 1(a)、(b)、(c)和(d)分别表示样品 1、2、3 和 4 中 In 组分随 InAlAs 缓冲层厚度变化

vious cross-hatch pattern, which could be attributed to the two types of misfit dislocations A and B oriented along the [1-10] and [110] directions, corresponding to group V and III atom based cores, respectively. From Figs. 2(a) and 2(b), it seems that there are less ridges along the [1-10] direction in the surface of sample 2 than that of sample 1. The root mean square (RMS) roughness value is 16.1 nm for sample 2 with compositional overshoot, slightly smaller than 18.8 nm for sample 1. For the $In_{0.84}Ga_{0.16}As$ PD samples, the RMS value is 12.6 nm for sample 4, also slightly smaller than 14.5 nm for sample 3. However, it is not sufficient to evaluate the sample quality only by surface morphologies.

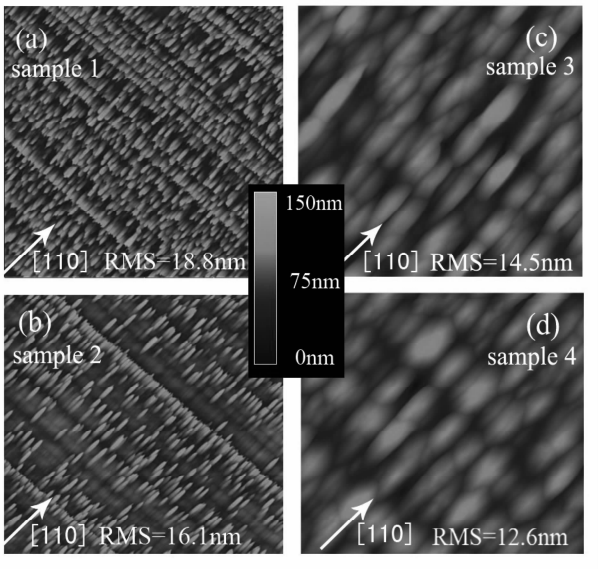

Fig. 2 The AFM images of (a) sample 1, (b) sample 2, (c) sample 3, and (d) sample 4
图2 各样品的AFM图样 (a)样品1,(b)样品2,(c)样品3,(d)样品4

The measured X-ray diffraction RSM of sample 1 is shown in Fig. 3, and the RSM images of other samples show similar patterns. The intensities are in logarithmic scale, the relative narrow and circular peak corresponds to the InP substrate (denoted as S), and the wide and elliptical peak corresponds to the epitaxy structures on the metamorphic InAlAs buffer (denoted as L). There are significant diffuse scatterings perpendicular to the normal line mainly owing to the existence of dislocations.[4] On the (004) reflections, the divergence of the centers of substrate peak and layer peak along the horizontal direction corresponds to the macroscopic tilt angle of the layers to the substrate. Some important parameters that could be extracted from the RSMs image are listed in Table 1.

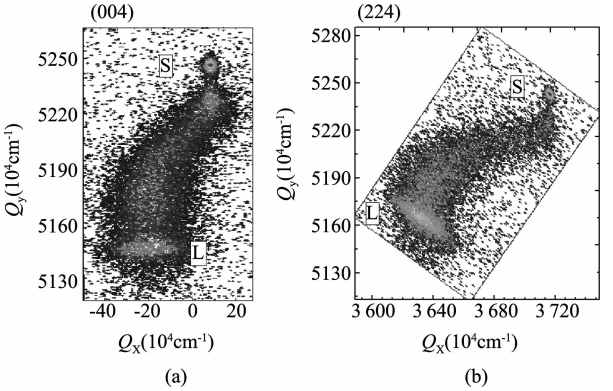

Fig. 3 The RSM of $In_{0.78}Ga_{0.22}As/In_{0.78}Al_{0.22}As$ QW sample 1 on InAlAs graded buffer. (a) along (004) direction, and (b) along (224) direction
图3 InAlAs 递变缓冲层上 $In_{0.78}Ga_{0.22}As/In_{0.78}Al_{0.22}As$ 量子阱结构样品1的倒易空间衍射图(a)X射线(004)面衍射,(b)X射线(224)面衍射

Table 1 Results from RSM measurements for samples 1~4
表1 从RSM测试中提取的4个样品的参数结果

Samples	Indium content	Cubic Mismatch (%)	Parallel Mismatch (%)	Perpendicular Mismatch (%)	Tilting Angle /(°)	Relax. Degree (%)	Residual Strain (10-3)
1	0.774	1.675	1.459	1.510	0.194	87.2	-2.13
2	0.781	1.730	1.716	2.006	-0.473	96.5	-0.60
3	0.838	2.125	2.069	2.324	-0.289	97.4	-0.54
4	0.840	2.136	2.095	2.288	-0.291	99.4	-0.45

The definition of degree of relaxation R for a layer is the ratio of parallel lattice mismatch $\delta a_{//}$ to the cubic lattice mismatch δa_∞, i.e. $R = \delta a_{//}/\delta a_\infty$. The cubic mismatch means the fractional difference of the unit cell lattice constants between the undistorted layer and substrate. It could be calculated from the perpendicular and parallel mismatch $\delta a_{//}$ and $\delta a_\perp$, and follows the form $\delta a_\infty = (\delta a_\perp + 2\delta a_{//} c_{12}/c_{11})/(1 + 2c_{12}/c_{11})$, where c_{11} and c_{12} are the elastic constants of the layer. And the residual strain can be also obtained from the formula $\varepsilon = (a_{//} - a_\infty)/a_\infty$. The tilting angle is the angle between the substrate and the epi-layer surfaces.

As shown in Table 1, the relaxation degree is 87.2% for sample 1, whereas is increased to 96.5% for sample 2. The error in determining the degree of relaxation as well as other parameters can be minimized

by doing more symmetric and asymmetric scans for the same sample on different direction. The manual peak defining may also cause some error but less than 1% during analyzing the RSM data in most cases. The residual strain is -2.13×10^{-3} for sample 1 and -6.0×10^{-4} for sample 2, respectively. The use of compositional overshoot in the $In_xAl_{1-x}As$ graded buffer favors the full relaxation and the release of residual strain in $In_{0.78}Ga_{0.22}As/In_{0.78}Al_{0.22}As$ QWs. In the case of $In_{0.84}Ga_{0.16}As$ PD structures, the relaxation degrees are larger than 95% for both samples 3 and 4, and the residual strain are both approximately -5.0×10^{-4}. The not obvious difference between samples 3 and 4 is probably owing to the much thicker epilayers on the $In_xAl_{1-x}As$ metamorphic graded buffers compared to samples 1 and 2. For sample 4 with compositional overshoot in the InAlAs buffer, it is believed that the residual strain has fully released after the growth of buffer layer, and for sample 3 there is still some residual strain after the growth of buffer layer and it releases gradually during the growth of absorption layer, though the final results show little difference between the two samples. Therefore, it can be concluded that the structural properties are markedly improved by using the compositional overshoot for the thinner QW structures, while for the relative thick PD structures no obvious improvement could be observed by HRXRD measurement.

The RT PL spectra of the four samples are shown in Fig. 4. For the two QW samples, the PL peak energies are both approximately at 2.2 μm. The PL intensity of sample 2 is slightly stronger than that of sample 1 as shown in Fig. 4. It indicates that the optical properties of the QW sample 2 are improved and there are less defects in the QWs of sample 2 after using the compositional overshoot in the graded buffer. It can be seen that the PL intensity of the two $In_{0.84}GA_{0.16}As$ PD samples are very close. It indicates that the effects of compositional overshoot for thicker PD structures are not as significant as in the case for thinner metamorphic QW samples.

3 Conclusions

In conclusion, the effects of compositional overshoot in InP-based $In_xAl_{1-x}As$ metamorphic graded buffers on the material qualities of $In_{0.78}Ga_{0.22}As/In_{0.78}Al_{0.22}As$ QW and $In_{0.84}GA_{0.16}As$ PD samples were investigated. The AFM results show that the compositional overshoot in the InAlAs buffer layers reduces the surface roughness for both QW and PD samples. HRXRD RSM and PL measurements show that the use of compositional overshoot increases the relaxation degree, reduces the residual strain, and enhances the optical quality in the case of thin QWs. On the other hand, no obvious difference is observed by HRXRD and PL measurements in the case of thick PDs. The different performances of the metamorphic QW and PD structures need to be considered in the device applications.

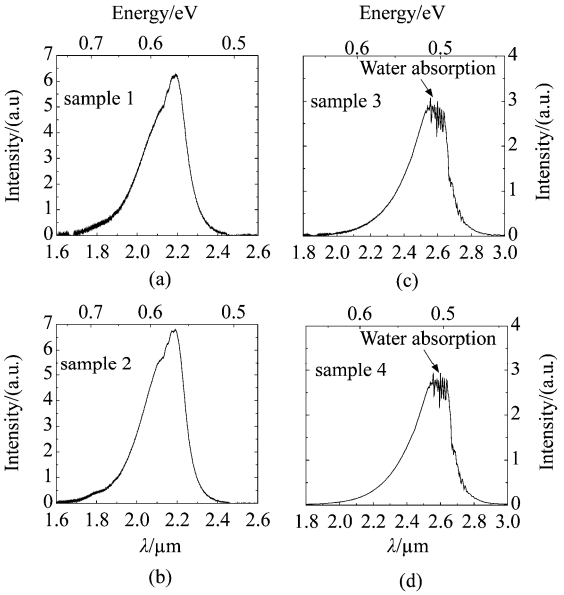

Fig. 4　The RT PL spectra of (a) sample 1, (b) sample 2, (c) sample 3, and (d) sample 4
图 4　室温光致发光谱 (a)样品 1,(b)样品 2,(c)样品 3,(d)样品 4

REFERENCES

[1] Arai M, Tadokoro T, Fujisawa T, *et al*. Uncooled (25 ~ 85℃) 10 Gbit/s operation of 1.3 μm-range metamorphic Fabry-Perot laser on GaAs substrate [J]. *Electron. Lett.*, 2009, **45**(7): 359 - 360.

[2] Lee B, Baek J H, Lee J H, *et al*. Optical properties of InGaAs linear graded buffer layers on GaAs grown by metalorganic chemical vapor deposition [J]. *Appl. Phys. Lett.*, 1996, **68**(21): 2973 - 2975.

[3] Gu Y, Zhang Y G., Wang K, *et al*. InP-based InAs/In-

(下转第 490 页)

and methane based on TDLAS near 1.626 μm. The determined characteristic peak positions from previous investigations and available databases are reasonable for separating the mixed gas absorption line. A measurement accuracy of 5% can be achieved as verified with the standard sample of mixed controlled concentrations.

REFERENCES

[1] Schoor F V, Verplaetsen E, Berghmans J. Calculation of the upper flammability limit of methane/air mixtures at elevated pressures and temperatures[J]. *J. Hazard. Mater.*, 2008, **153**(3):1301-1307.

[2] Rice C A, Perram G. A tunable diode laser absorption system for long path atmospheric transmission and high energy laser applications[C]. *In atmospheric and oceanic propagation of electromagnetic waves V*, *SPIE*, 2011:7924.

[3] Polson D, Fowler D, Nemitz E, *et al*. Estimation of spatial apportionment of greenhouse gas emissions for the UK using boundary layer measurements and inverse modelling technique[J]. *Atmos. Environ.*, 2011, **45**(4):1042-1049.

[4] Giubileo G, Dominicis L D, Fantoni R, *et al*. Photoacoustic detection of ethylene traces in biogenic gases[J]. *Laser Phys.*, 2002, **12**(4):653-655.

[5] Basu S, Lambe D E, Kumar R. Water vapor and carbon dioxide species measurements in narrow channels[J]. *Int. J. Heat Mass Transfer*, 2010, **53**(4):703-714.

[6] Adamus A, Sancer J, Guranova P, *et al*. An investigation of the factors associated with interpretation of mine atmosphere for spontaneous combustion in coal mines[J]. *Fuel Process. Technol.*, 2011, **92**(3):663-670.

[7] Hendricks A G, Vandsburger U, Saunders W R, *et al*. The use of tunable diode laser absorption spectroscopy for the measurement of flame dynamics[J]. *Meas. Sci. Technol.*, 2006, **17**(1):139-144.

[8] Puiu A, Giubileo G, Bangrazi C. Laser sensors for trace gases in human breath[J]. *Intern. J. Environ. Anal. Chem.*, 2005, **85**(12-13):1001-1012.

[9] McCulloch M T, Langford N, Duxbury G. Real-time trace-level detection of carbon dioxide and ethylene in car exhaust gases[J]. *Appl. Opt.*, 2005, **44**(14):2887-2894.

[10] Boschetti A, Bassi D, Iacob E, *et al*. Resonant photoacoustic simultaneous detection of methane and ethylene by means of a 1.63-μm diode laser[J]. *Appl. Phys. B*, 2002, **74**(3):273-278.

[11] Harward C N, Thweatt W D, Baren R E, *et al*. Determination of molecular line parameters for acrolein(C3H4O) using infrared tunable diode laser absorption spectroscopy[J]. *Spectrochim. Acta. Part A*, 2006, **63**(5):970-980.

[12] Krzempek K, Lewicki R, Nahle L, *et al*. Continuous wave, distributed feedback diode laser based sensor for trace-gas detection of ethane[J]. *Appl. Phys. B*, 2012, **106**(2):251-255.

[13] Duraev V P, Marmalyuk A A, Petrovskiy A V. Tunable laser diodes for the 1250 ~ 1650 nm spectral range[J]. *Spectrochim. Acta. Part A*, 2007, **66**(4-5):846-848.

[14] Guan Z, Lewander M, Svanberg S. Quasi zero-background tunable diode laser absorption spectroscopy employing a balanced Michelson interferometer[J]. *Opt. Express*, 2008, **16**(26):21714-21720.

[15] Brown D M, Shi K B, Liu Z W, *et al*. Long-path supercontinuum absorption spectroscopy for measurement of atmospheric constituents[J]. *Opt. Express*, 2008, **16**(12):8457-8471.

[16] Mazzotti D, Giusfredi G, Cancio P, *et al*. High-sensitivity spectroscopy of CO_2 around 4.25 μm with difference-frequency radiation[J]. *Opt. Laser Eng*, 2002, **37**(2):143-158.

[17] Rothman L S, Gordon I E, Barbe A, *et al*. The HITRAN 2008 molecular spectroscopic database[J]. *J. Quant. Spectrosc. Radiat. Transfer*, 2009, **110**(40462):533-572.

(上接485页)

GaAs quantum wells with type-I emission beyond 3μm[J]. *Appl. Phys. Lett.*, 2011, **99**(8): 081914.

[4] Hudait M K, Lin Y, Ringel S A. Strain relaxation properties of $InAs_yP_{1-y}$ metamorphic materials grown on InP substrates[J]. *J. Appl. Phys*, 2009, **105**(6): 061643.

[5] Kirch J, Garrod T, Kim S, *et al*. $InAs_yP_{1-y}$ metamorphic buffer layers on InP substrates for mid-IR diode lasers[J]. *J. Cryst. Growth*, 2010, **312**(8): 1165 - 1169.

[6] Tångring I T, Wang S M, Zhu X R, *et al*. Manipulation of strain relaxation in metamorphic heterostructures[J]. *Appl. Phys. Lett*, 2007, **90**(7): 071904.

[7] Song Y X, Wang S M, Lai Z H, *et al*. Enhancement of optical quality in metamorphic quantum wells using dilute nitride buffers[J]. *Appl. Phys. Lett*, 2010, **97**(9): 091903.

[8] Yang J, Bhattacharya P, Mi Z. High-performance $In_{0.5}Ga_{0.5}As$/GaAs quantum-dot lasers on silicon with multiple-layer quantum-dot dislocation filters[J]. *IEEE Trans. Electron Devices* 2007, **54**(11): 2849 - 2855.

[9] Gu Y, Zhang Y G., Wang K, *et al*. InAlAs graded metamorphic buffer with digital alloy intermediate layers[J]. *Jpn. J. Appl. Phys*, 2012, **51**(8): 080205.

[10] Tersoff J. Dislocations and strain relief in compositionally graded layers[J]. *Appl. Phys. Lett.*, 1993, **62**(7): 693 - 695.

[11] Zhang Y G., Gu Y, Wang K, *et al*. Properties of gas source molecular beam epitaxy grown wavelength extended InGaAs photodetectors structures on linear graded InAlAs buffer[J]. *Semicon. Sci. Technol*, 2008, **23**(12): 125029.

[12] Lee D, Park M S, Tang Z, *et al*. Characterization of metamorphic $In_xAl_{1-x}As$/GaAsbuffer layers using reciprocal space mapping[J]. *J. Appl. Phys*, 2007, **101**(6): 063523.

[13] Choi H, Jeong Y, Cho J, *et al*. Effectiveness of non-linear graded buffers for In(Ga, Al)As metamorphic layers grown on GaAs (0 0 1)[J]. *J. Cryst. Growth*, 2009, **311**(4): 1091 - 1095.

[14] Wang K, Zhang Y G, Gu Y, *et al*. Improving the performance of extended wavelength InGaAs photodetectors by using digital graded hetero-interfaces superlattice[J]. J. Infrared Millim. Waves., 2009, **28**(6): 0405.